Surface Deformation Monitoring Using Polarimetric Time-series InSAR data

Yasser Maghsoudi

Associate Professor, Geomatics Engineering Faculty,

K. N. Toosi University of Technology

Introduction

The earth surface is affected by a wide range of deformation phenomena

Water extraction

Glaciers

Earthquakes and volcanoes

Landslides

Power plants

Mining

Oil and Gas

Infrastructures

Introduction

Land subsidence in Iran

The widespread water over-exploitation is the main cause of land subsidence in Iran.

Introduction

Subsidence effects

- Changes in topographic and hydrological characteristics of the area.
- loss of the aquifer capacity.
- Building and substructure destruction.
- Destruction of fertile soils which is a consequence of diminished porosity of soil.
- Sinkhole formation

Introduction

Hamekasi Sinkhole, Hamedan

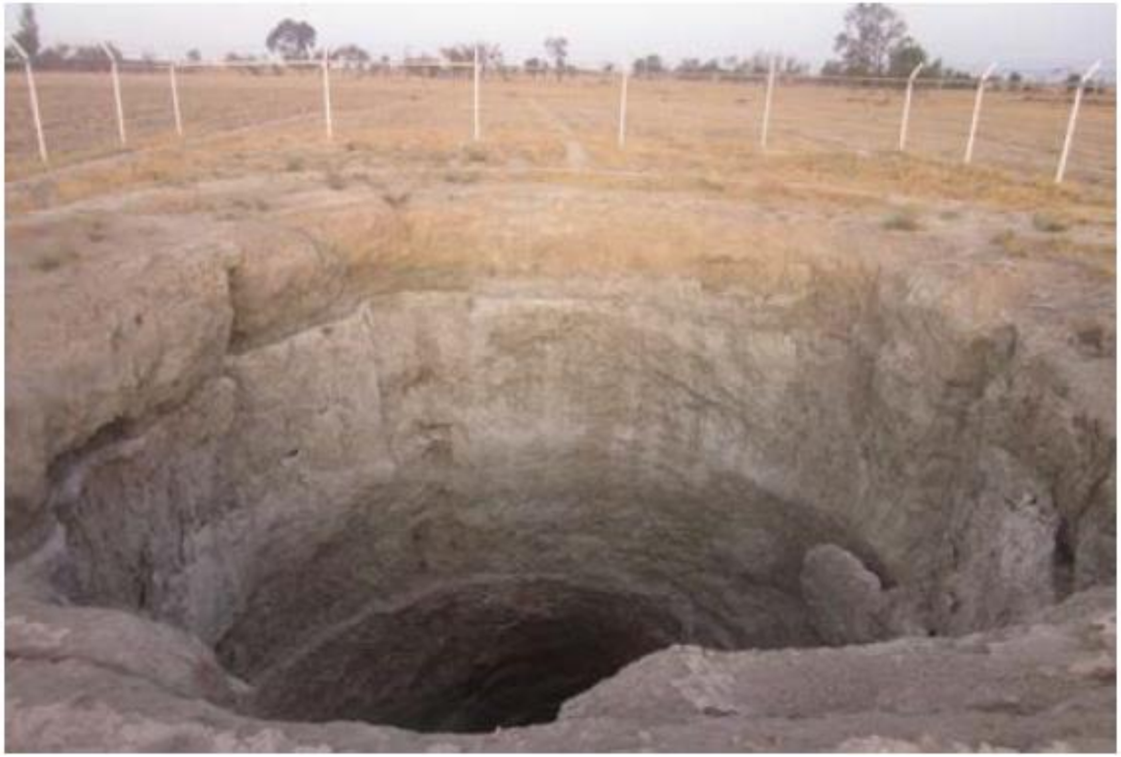

Introduction

Kabodarahand sinkhole, Hamedan

Introduction

Kerdabad sinkhole, Hamedan

Introduction

Land Subsidence Estimation Methods

- Ground-based
  - Precise Leveling
  - GPS

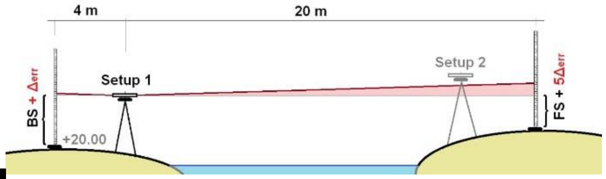

- Satellite-based
  - SAR Interferometry

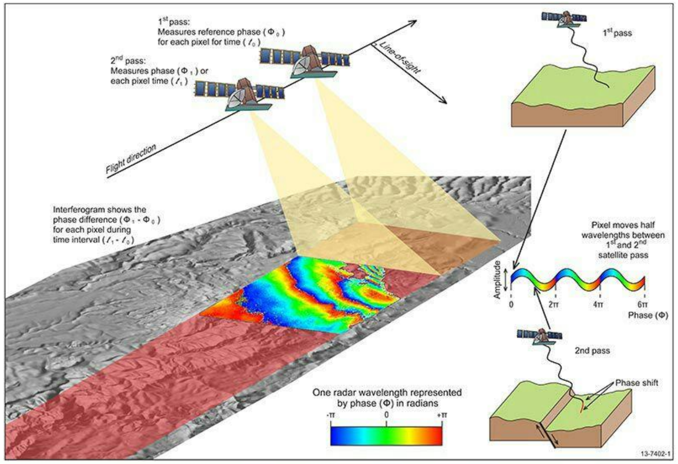

Repeat pass interferometry

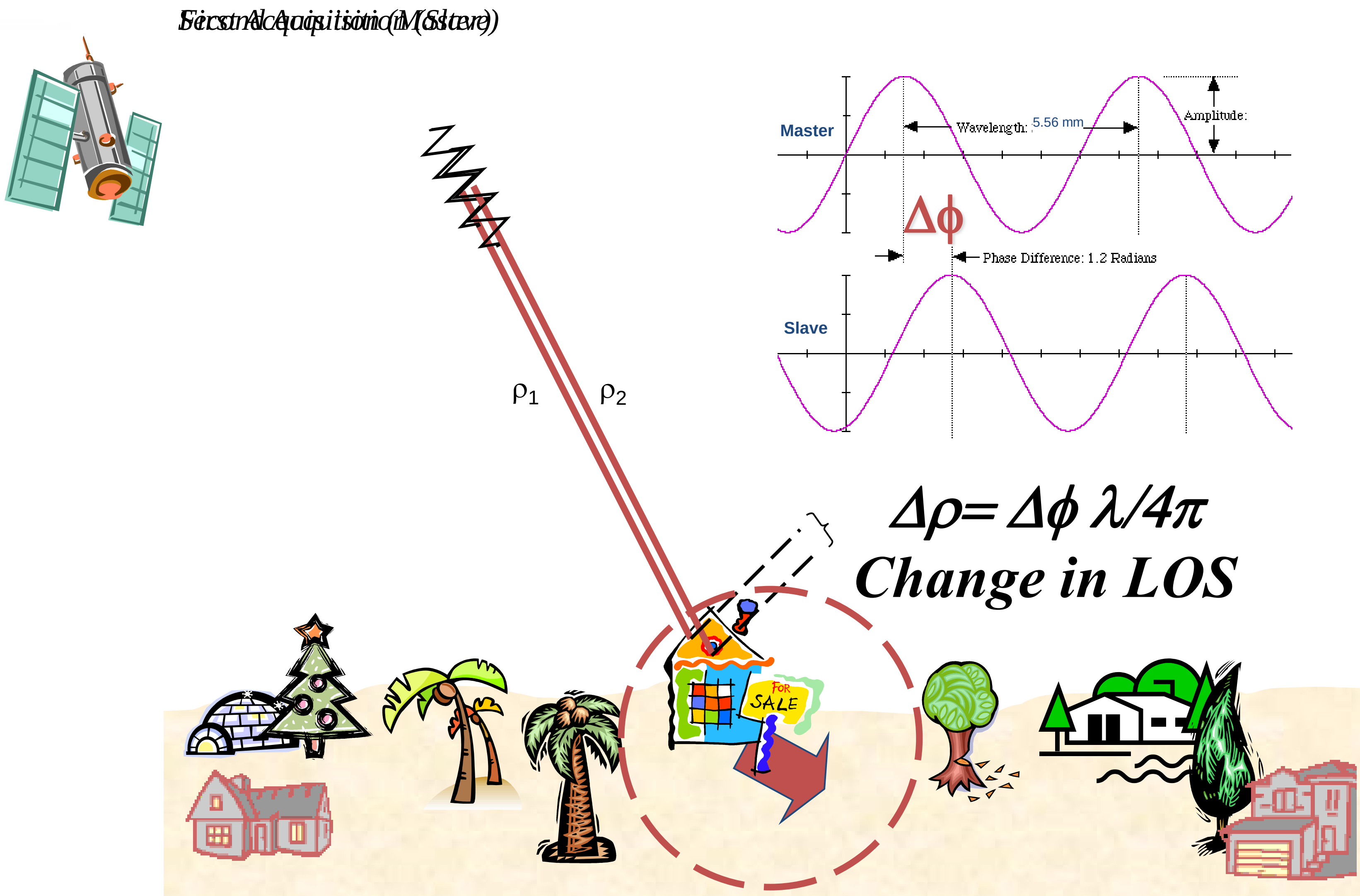

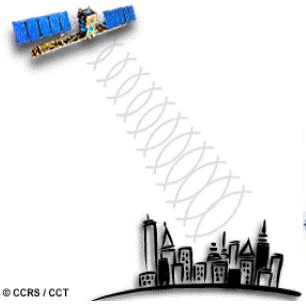

Introduction

- **The primary limitations of InSAR**

    - **Decorrelation**
    - **Small deformation signal**

Persistent Scatterer (PS)

The Persistent Scatterers Interferometry (PSI) technique can be used to analyze Time-series of SAR Images. The main goal of the PSI technique is the identification of image pixels, called permanent scatterers (PSs) in order to overcome the InSAR limitations. PS are corner reflector like resolution elements that are characterized by a dominant scatterer.

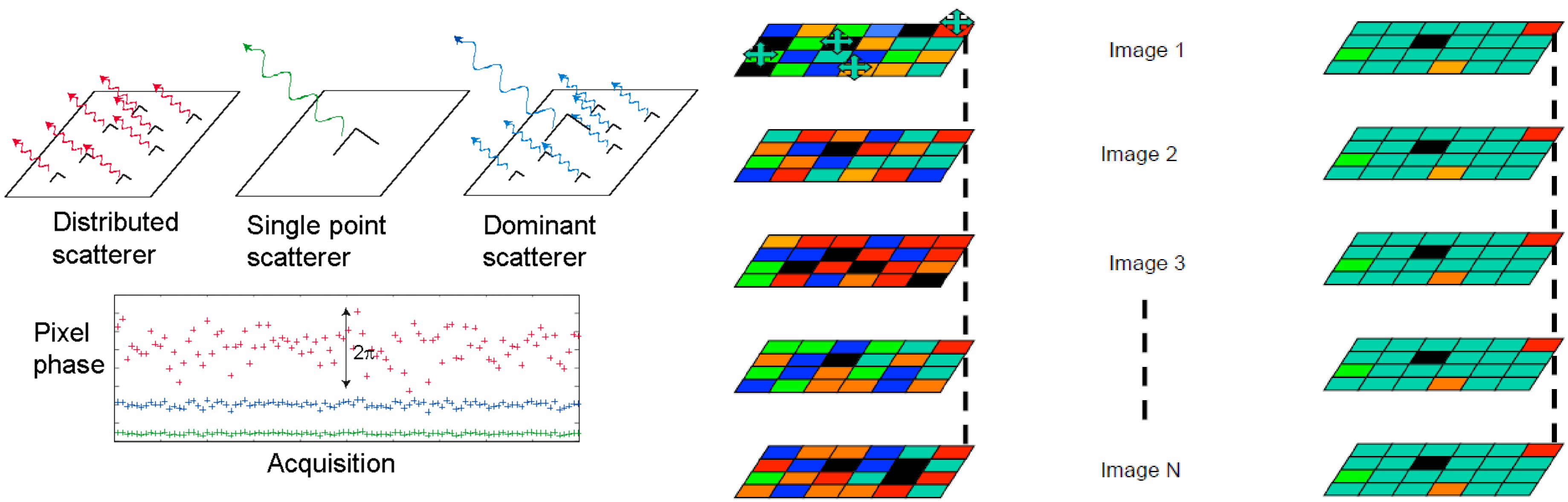

Land Subsidence:Varamin

Velocity map of **Varamin's plain**

Data : **Sentinel-1A**

Time period:
2014/19/10 to
2017/16/08

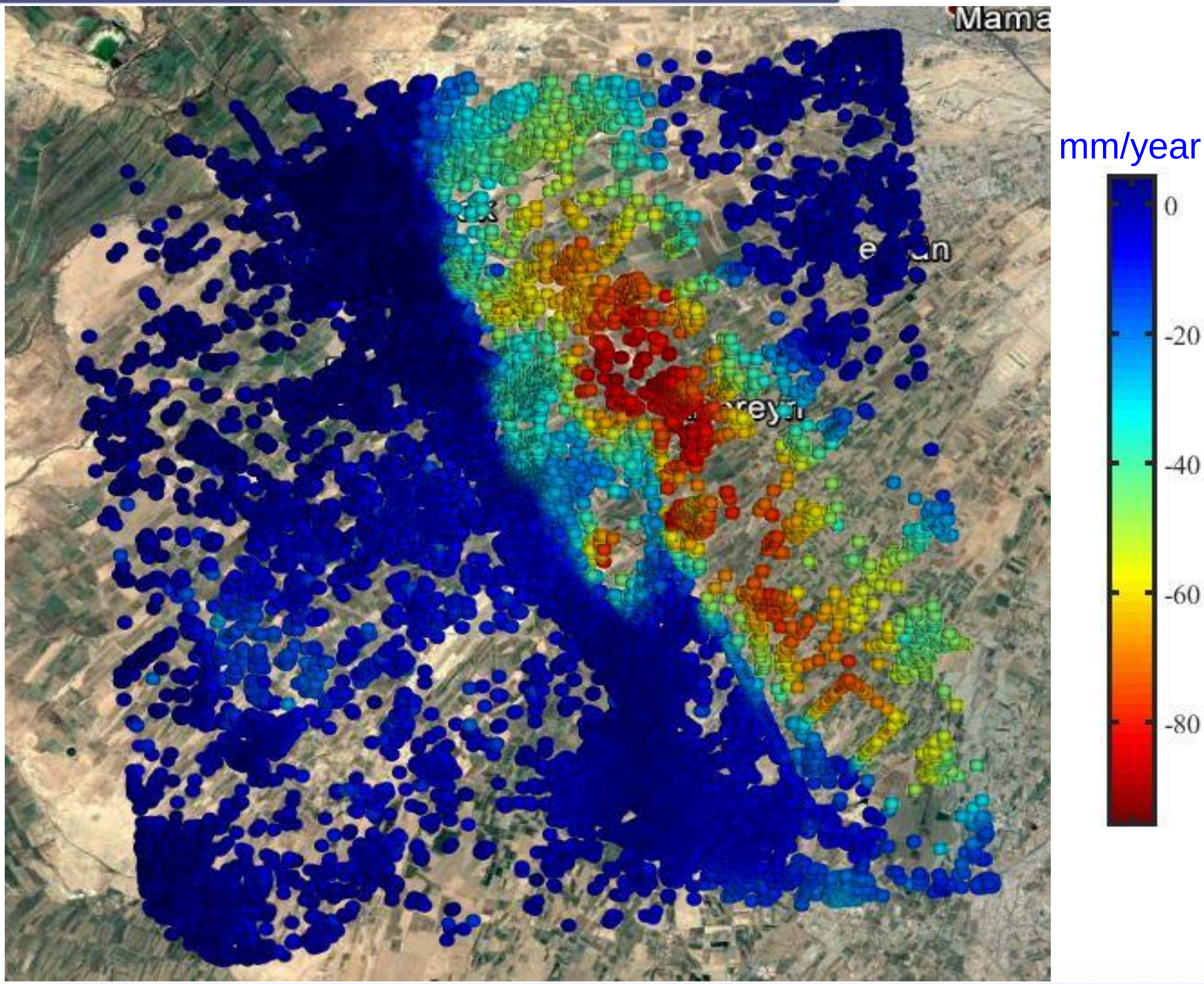

Land Subsidence: IKA

Velocity map of
IKA Airport

Data : **Sentinel-1A**

Time period:
2014/19/10 to
2017/16/08

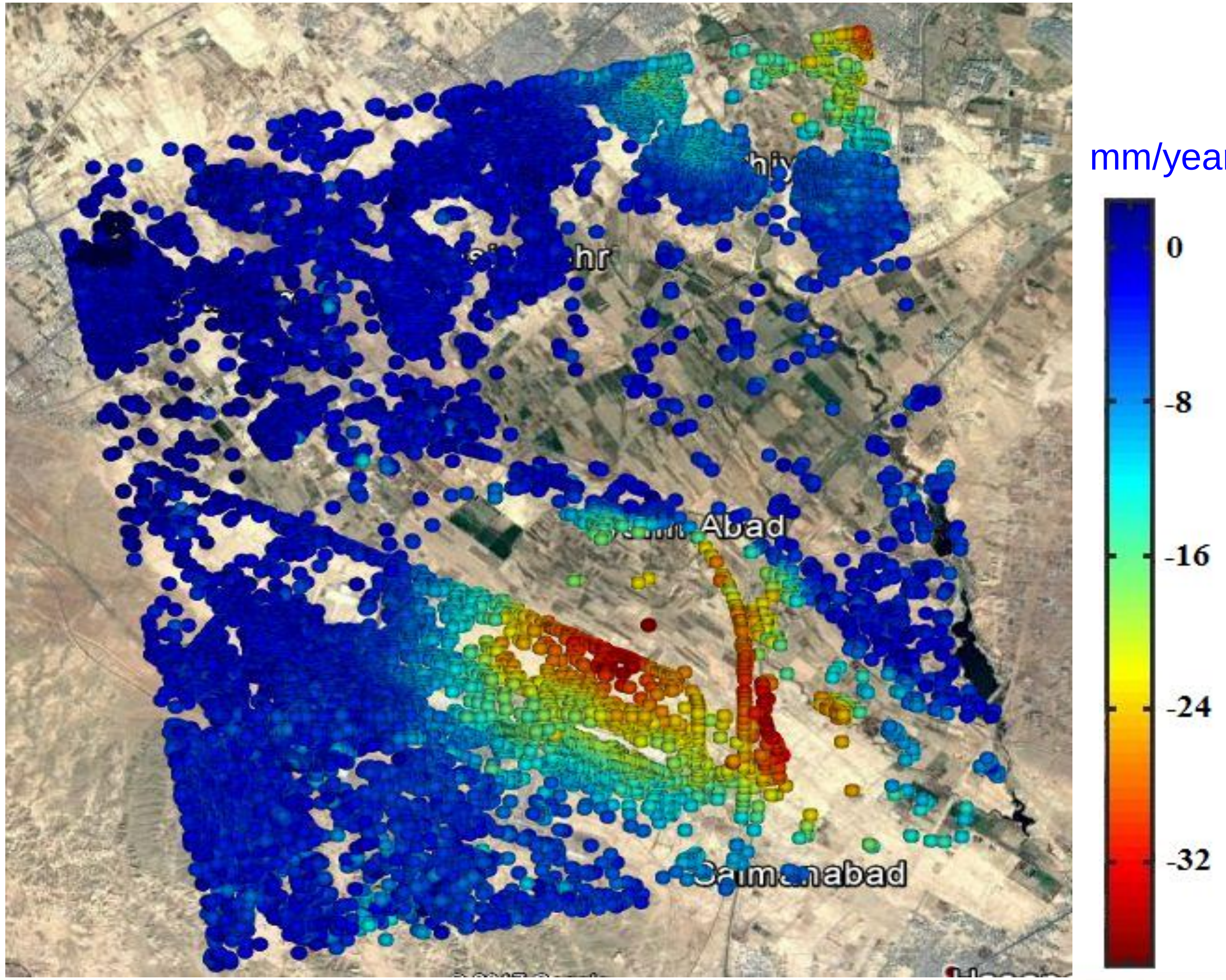

Land Subsidence: IKA

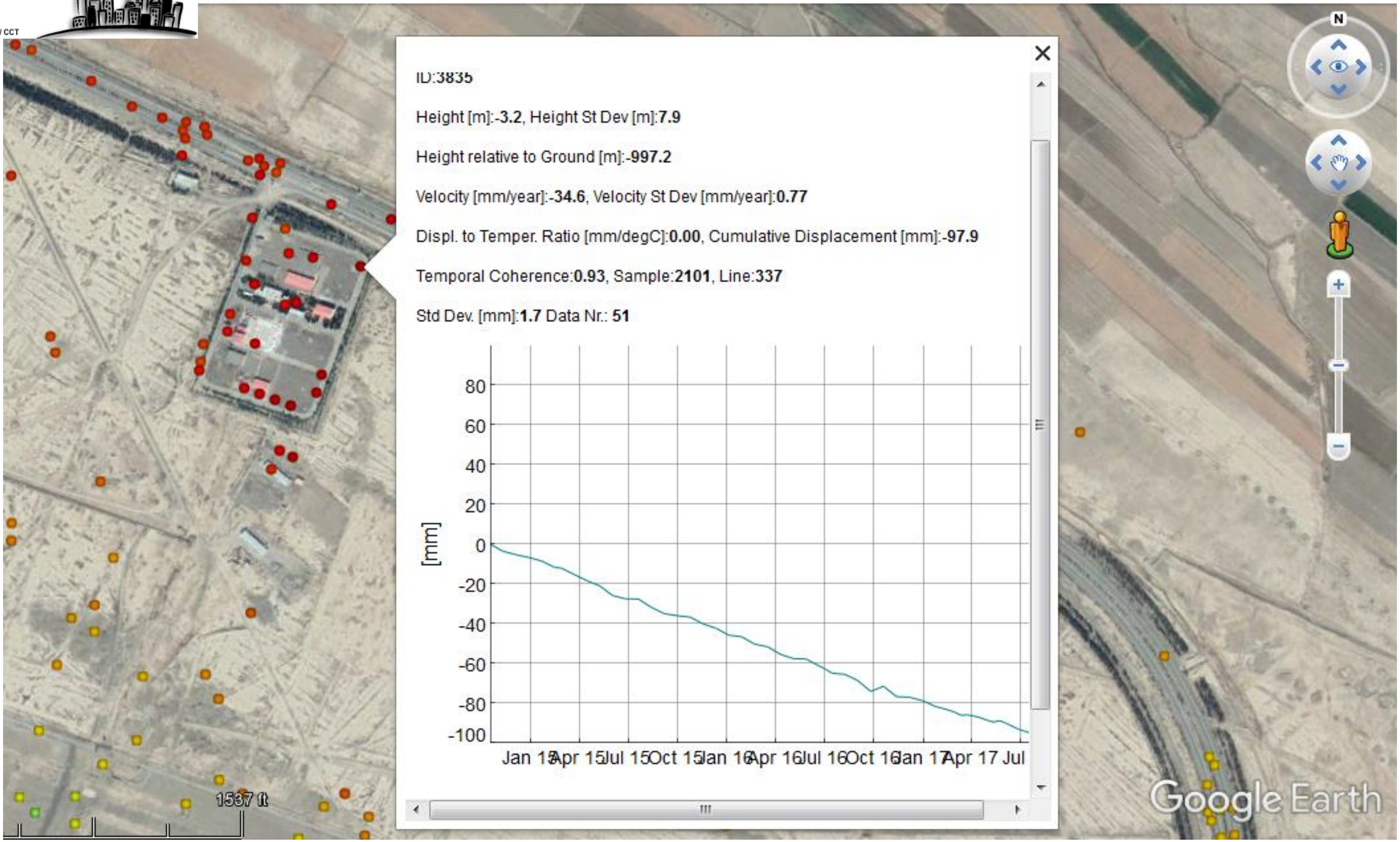

Land Subsidence: Tehran

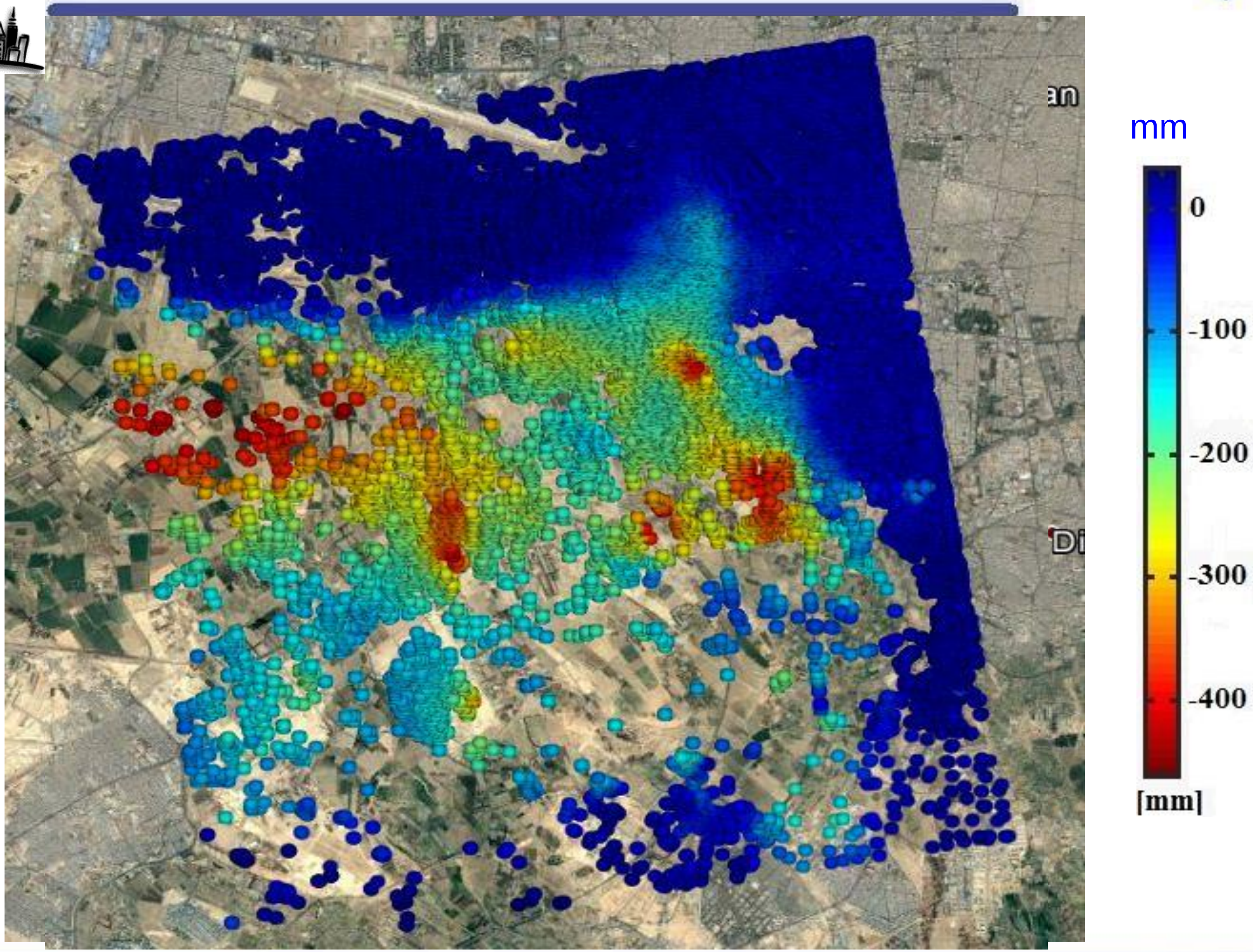

Land Subsidence: Tehran

Polarimetric InSAR: Motivations

© CCRS / CCT

- Persistent Scatterer Interferometry (PSI) is a powerful technique for monitoring urban areas, characterized by a high density of point-wise stable targets originated by man-made structures.
- All PSI algorithms struggle to provide high-quality measurements over non-urban areas.
- In the non-urban area, poor PS density is primarily associated with both temporal and geometrical decorrelation phenomena.

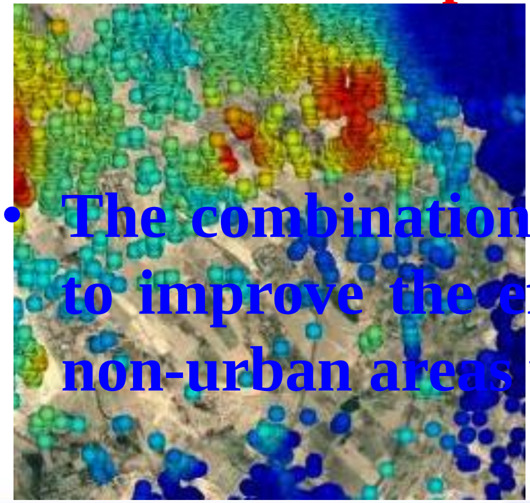

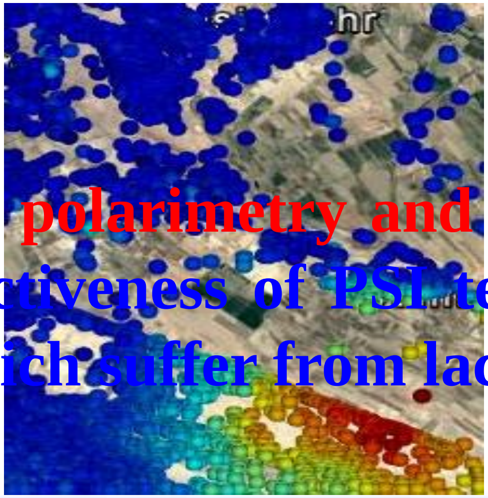

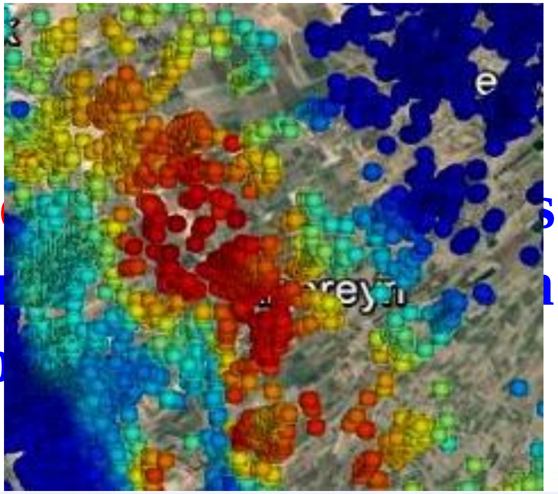

- The combination of polarimetry and int … s to improve the effectiveness of PSI techn … n non-urban areas which suffer from lack o

Polarimetric InSAR

Radar data polarization

- Single polarization
  - HH
  - VV
  - HV
  - VH
- Dual polarization
  - HH,VV
  - HH, HV
  - VV,VH
- Full polarization
  - HH, VV, HV or VH

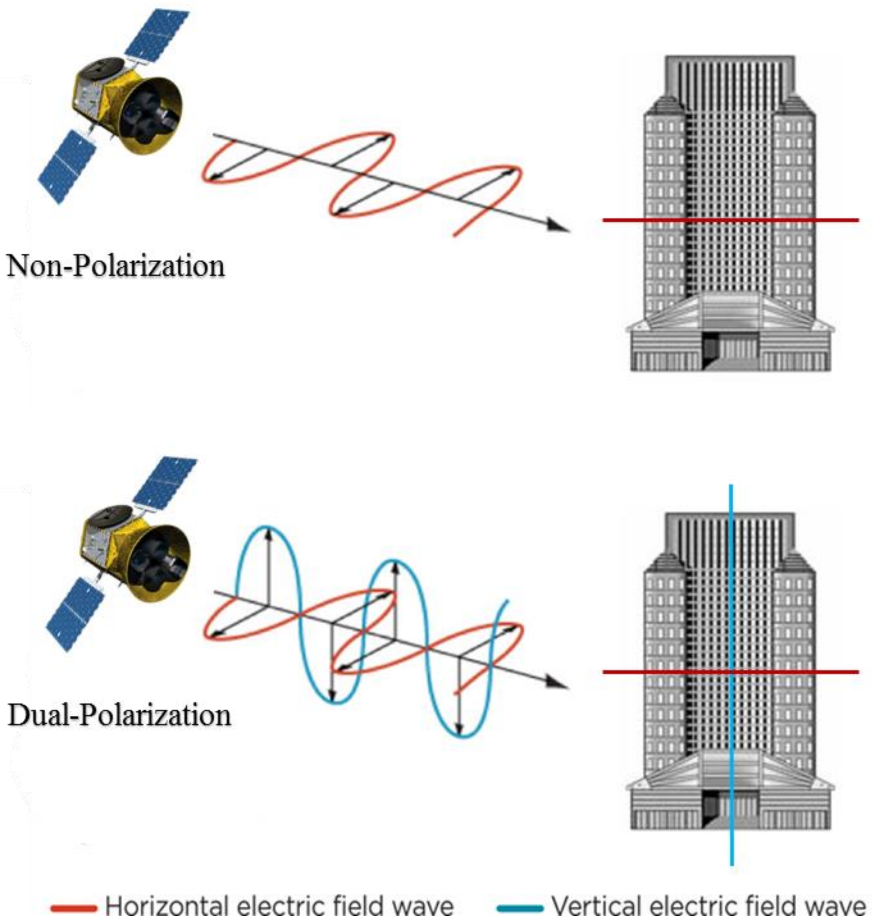

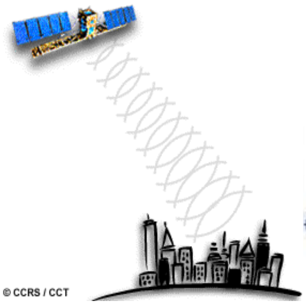

Polarimetric InSAR

Polarimetric SAR Interferometry (PolInSAR):

The combination of radar polarimetry and radar interferometry, known as PolInSAR, was first introduced by Cloude and Papathanassiou (Cloude and Papathanassiou, 1997).

Polarimetric + Interferometry = PolInSAR

$$S \xrightarrow{\quad\quad\quad\quad\omega\quad\quad\quad\quad} \mu$$

$$\mu = \left(\underline{\omega}^{*T} \underline{k} \right)$$

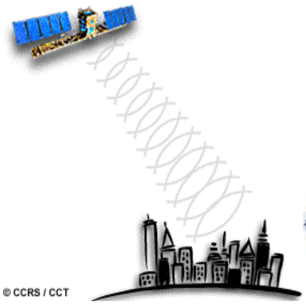

Polarimetric InSAR

$$\mu = \left(\underline{\omega}^{*T}\underline{k}\right)$$

$$S = \begin{bmatrix} S_{hh} & S_{hv} \\ S_{vh} & S_{vv} \end{bmatrix}$$

$$\underline{\omega} = \begin{bmatrix} \cos\alpha \\ \sin\alpha\cos\beta\, e^{j\delta} \\ \sin\alpha\sin\beta\, e^{j\gamma} \end{bmatrix} = \begin{cases} 0 \le \alpha \le \dfrac{\pi}{2}; 0 \le \beta \le \pi \\ 0 \le \delta \le \pi; -\pi \le \gamma < \pi \end{cases}$$

$$\underline{\omega} = \left[\cos(\alpha), \sin(\alpha)\, e^{j\Psi}\right]^T, \begin{cases} 0 \le \alpha \le \dfrac{\pi}{2} \\ -\pi \le \Psi \le \pi \end{cases}$$

$$\underline{\mathbf{k}} = \frac{1}{\sqrt{2}}\left[\mathrm{S_{hh}} + \mathrm{S_{vv}}, \mathrm{S_{hh}} - \mathrm{S_{vv}}, 2\mathrm{S_{hv}}\right]^{\mathrm{T}}$$

$$\underline{k} = \frac{1}{\sqrt{2}}\left[S_{hh} + S_{vv}, S_{hh} - S_{vv}\right]^T$$

$$\underline{k} = \left[S_{vv}, 2S_{vh}\right]^T$$

The main purpose of the polarimetric optimization consists of a search over the available polarimetric space, for each pixel, in order to find ω that optimizes the quality criterion.

S. R. Cloude and K. P. Papathanassiou, “Polarimetric optimisation in radar interferometry,” *Electron. Lett.*, vol. 33, no. 13, pp. 1176–1178, Jun.1997.

Polarimetric Optimization

The proposed polarimetric optimization methods:

Amplitude-based polarimetric optimization

Amplitude Dispersion Index (ADI)

$$D_A = \frac{\sigma_a}{\bar{a}} = \frac{\sqrt{\frac{\sum_{i=1}^{N}(|s_i| - |\bar{s}|)^2}{N}}}{\frac{1}{N}\sum_{i=1}^{N}|s_i|}$$

Phase-based polarimetric optimization

Temporal Coherence (TC)

$$T_{C_x} = \frac{1}{N}\sum_{i=1}^{N}\left(\exp\{\sqrt{-1}\,(\varphi_{x,i} - \varphi_{\Delta h_{x,i}} - \varphi_{v_{x,i}} - \varphi_{\varepsilon_{x,i}})\}\right)$$

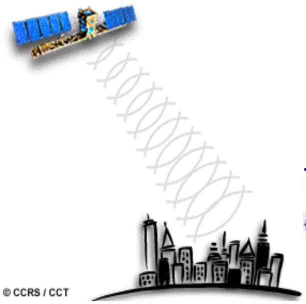

Polarimetric InSAR
Amplitude Dispersion Index Optimization

ADI optimization

$$D_A = \frac{\sigma_a}{\bar{a}} = \frac{\sqrt{\frac{\sum_{i=1}^{N}(|s_i| - |\bar{s}|)^2}{N}}}{\frac{1}{N}\sum_{i=1}^{N}|s_i|}$$

$$\mathbf{s} = \mu = \left(\underline{\omega}^{*T}\underline{k}\right)$$

$$D_{A\,Pol} = \frac{\sqrt{\frac{\sum_{\mathrm{i}=1}^{N}\left(\left|\underline{\omega}^{*T}\underline{k}_i\right| - \left|\overline{\underline{\omega}^{*T}\underline{k}}\right|\right)^2}{N}}}{\frac{1}{N}\sum_{\mathrm{i}=1}^{N}\left|\underline{\omega}^{*T}\underline{k}_i\right|}$$

The polarimetric form of ADI

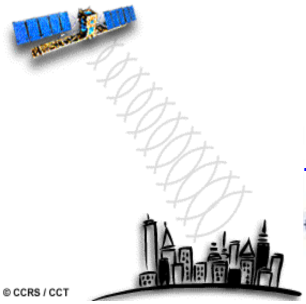

Polarimetric InSAR Amplitude Dispersion Index Optimization

STUDY AREA AND DATASET DESCRIPTION

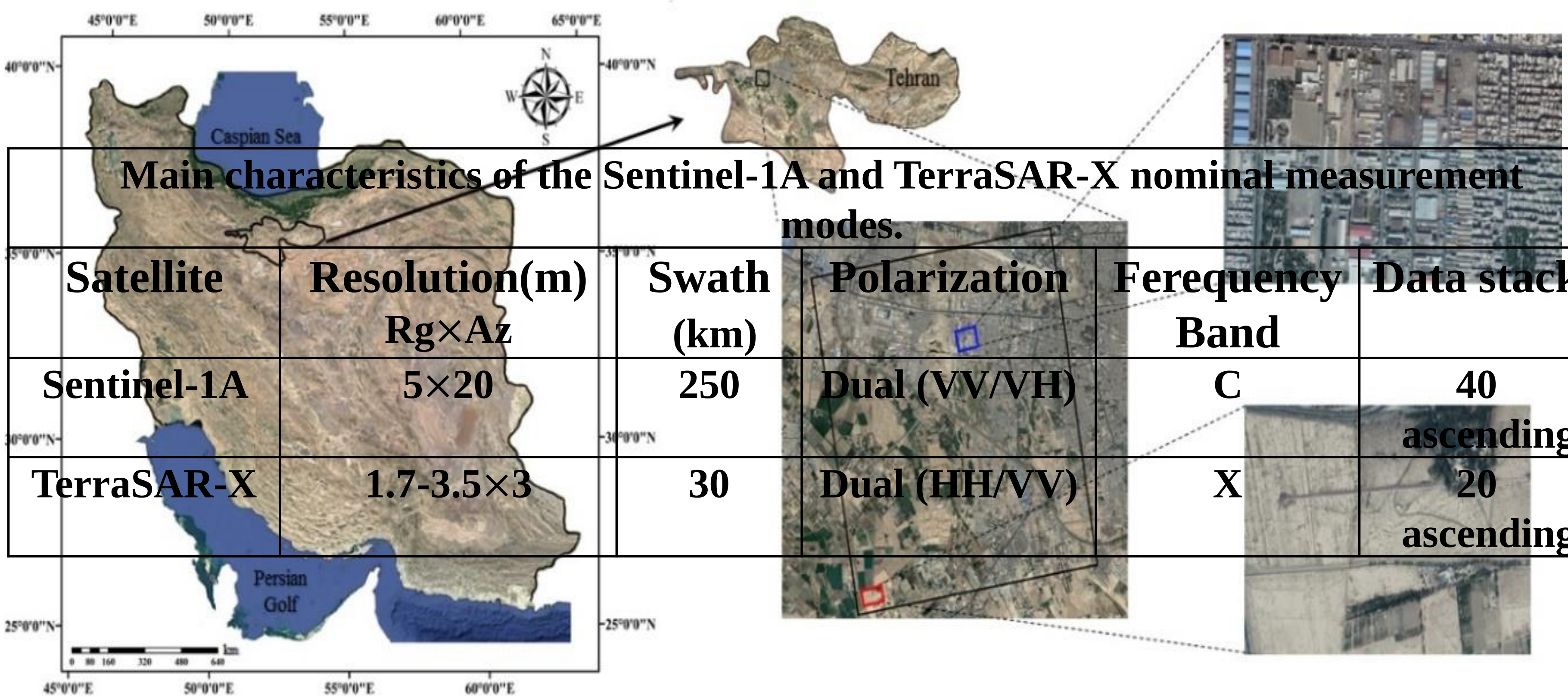

Main characteristics of the Sentinel-1A and TerraSAR-X nominal measurement modes.

Satellite	Resolution(m) Rg×Az	Swath (km)	Polarization	Ferequency Band	Data stack
Sentinel-1A	5×20	250	Dual (VV/VH)	C	40 ascending
TerraSAR-X	1.7-3.5×3	30	Dual (HH/VV)	X	20 ascending

Polarimetric InSAR
Amplitude Dispersion Index Optimization

Histogram of ADI values

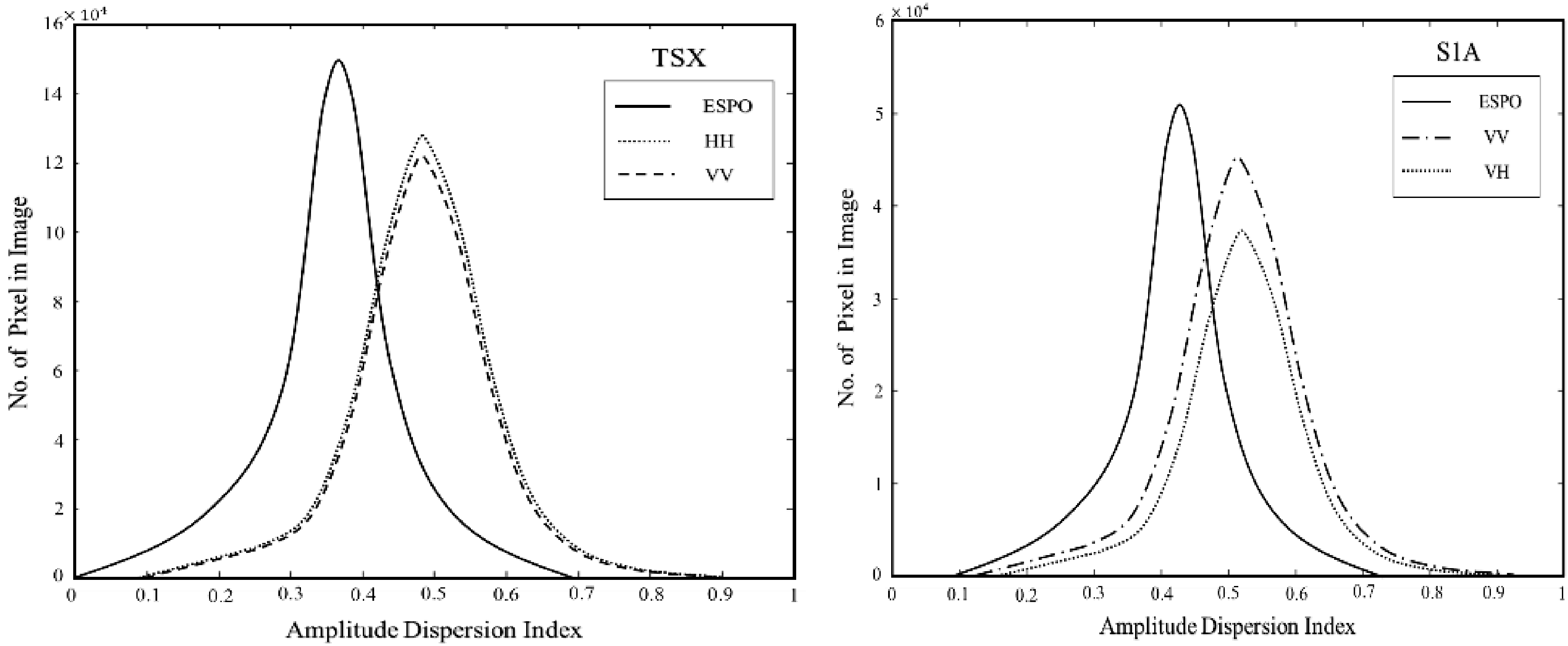

Polarimetric InSAR
Amplitude Dispersion Index Optimization

© CCRS / CCT

Number of detected PSC and PS pixels in S1A and TSX channels

Channel	Number of PSC pixels	Number of PS pixels
VV (S1A)	192256	168683
Opt (S1A)	382588	286821
HH (TSX)	465589	443131
VV (TSX)	408639	370394
Opt (TSX)	1516239	1287352

1.7 times
2 times

3 times
3.5 times

- Optimization methods are more effective in the PSC improvement than in increasing the PS numbers.
- The optimization method has been more successful for TSX data compared to S1A data

Polarimetric InSAR
Amplitude Dispersion Index Optimization

Close up view of PS pixels for S1A data

VV Channel | **Optimum Channel**

Non-urban

Urban

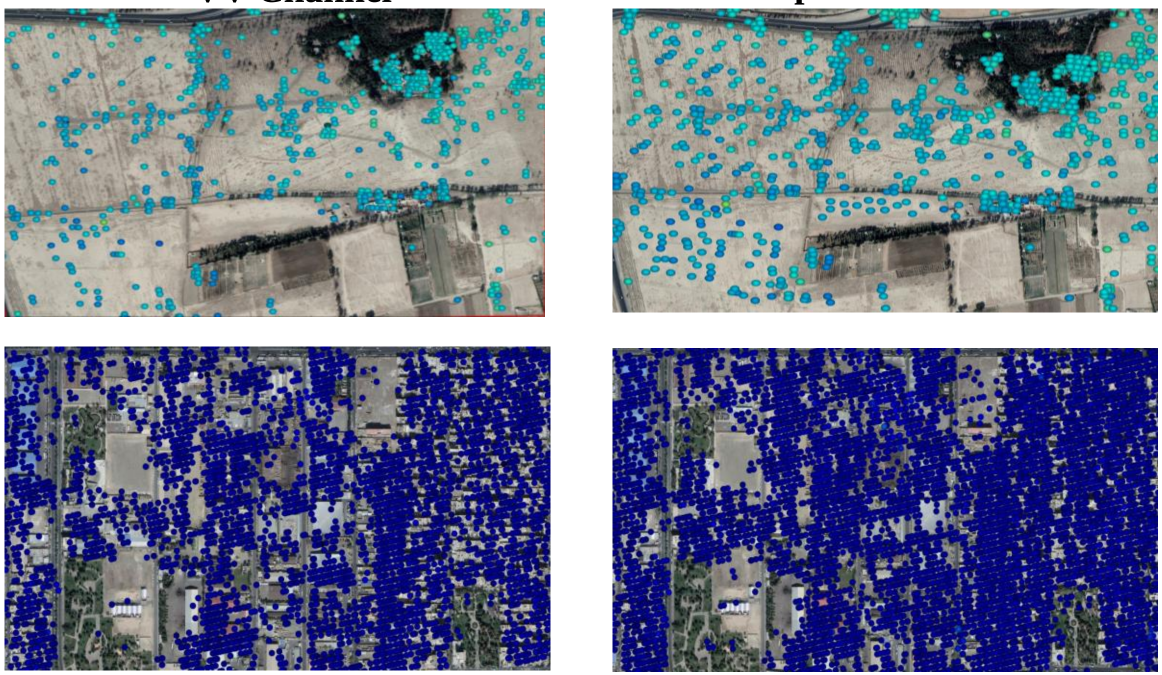

mm/year

Polarimetric InSAR
Temporal Coherence Optimization

Number of detected PS pixels in S1A channels

Channel	Number of PS pixels
VV	65767
Optimum	72124

10%

Deformation Results

Optimum channel **VV channel**

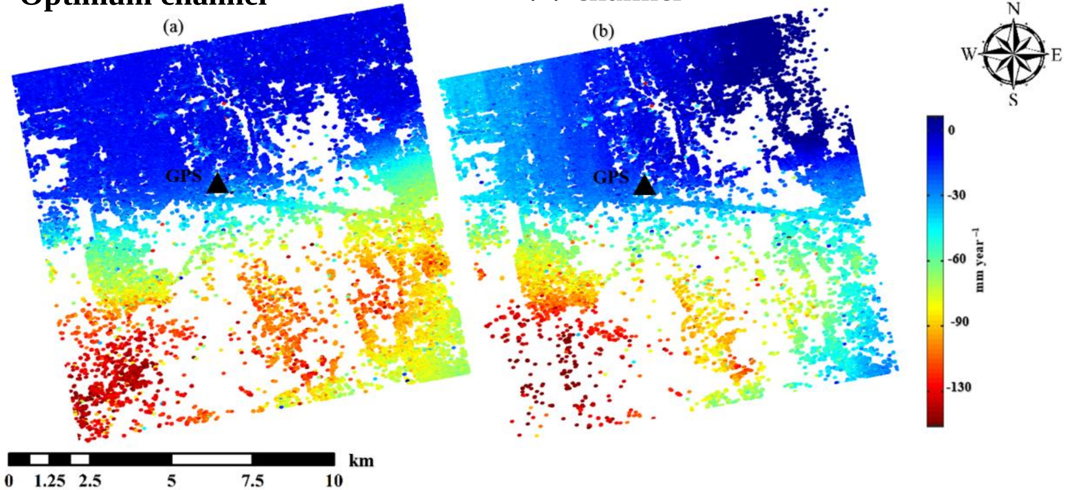

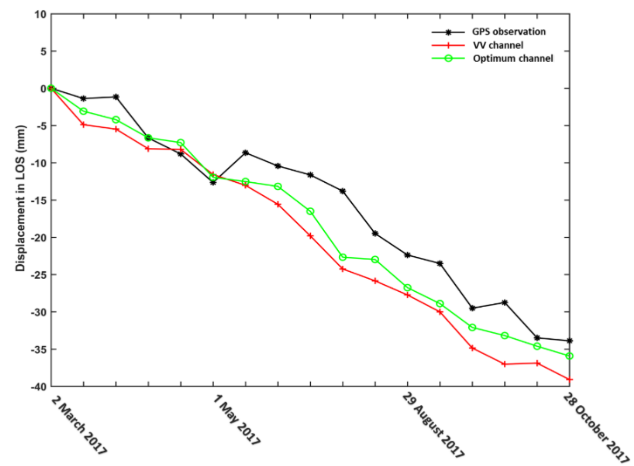

For more information :

Fatemeh Foroughnia, Sadegh Nemati, Yasser Maghsoudi and Daniele Perissin: *An Iterative PS-InSAR Method for the Analysis of Large Spatio-Temporal Baseline Data Stacks for Land Subsidence Estimation*. International Journal of Applied Earth Observation and Geoinformation, Feb 2019, 74, 248-258.

Saeed Azadnejad, Yasser Maghsoudi and Daniele Perissin: *Investigating the effect of the Physical Scattering Mechanism of the Dual-Polarization Sentinel-1 data on the Temporal Coherence Optimization results*. International Journal of Remote sensing, 03/2019; in press.

Evaluation of Polarimetric Capabilities of Dual polarized Sentinel-1 and TerraSAR-X data to improve the PSInSAR Algorithm using Amplitude Dispersion Index Optimization, International Journal of Applied Earth Observation and Geoinformation, 2019, In Press.

Mohammad Khorrami, Babak Alizadeh, Erfan Ghasemi Tousi, Mahyar Shakerian, Yasser Maghsoudi and Peyman Rahgozar: How Groundwater Level Fluctuations and Geotechnical Properties Lead to Asymmetric Subsidence: A PSInSAR Analysis of Land Deformation over a Transit Corridor in the Los Angeles Metropolitan Area. Remote Sens. 2019, 11(4), 377; DOI:10.3390/rs11040377